PROCEEDINGS OF SCIENCE

Impact of modified characteristics of hadronic interactions on cosmic-ray observables for proton and nuclear primaries

Jan Ebr,[a,*] **Jiří Blažek,**[a] **Jakub Vícha,**[a] **Tanguy Pierog,**[b] **Eva Santos,**[a] **Petr Trávníček**[a] **and Nikolas Denner**[a]

[a] *FZU - Institute of Physics of the Czech Academy of Sciences, Na Slovance 2, Prague, Czech Republic*

[b] *Karlsruhe Institute of Technology 76131 Karlsruhe, Germany*

E-mail: ebr@fzu.cz

Having implemented the option to make ad-hoc modifications of cross-section, multiplicity, and elasticity of hadronic interactions during the development of cosmic-ray showers into the CORSIKA simulation package in a consistent way for both primary protons and arbitrary nuclei, we can study the impact of these modifications on a variety of observables for different primaries. The modifications of the interactions are generic, without any reference to a specific mechanism. The ranges of parameters are only restricted by existing experimental data from accelerators and nuclear emulsions. The complete 3-dimensional view of the showers provided by CORSIKA allows us to study not only the depth of the maximum of the longitudinal development of the showers and total particle yield at the ground but also to see how the modifications impact the signal at different distances from the shower core and at different energy thresholds for the detection of secondary particles at the ground. Furthermore, we investigate the changes in the maximum depth where muons are produced, the expected rates of anomalous shower profiles, the correlation between the maximum of the longitudinal profiles and ground signal, and the fluctuations of all the observables. We show not only which modifications help the most to alleviate the tension between the current hadronic interaction models and data from ultra-high energy cosmic ray observatories, most prominently the Pierre Auger Observatory, but also which observables are the most sensitive to the individual parameters of the hadronic interactions, thus helping to guide the design of future cosmic-ray observatories.

38th International Cosmic Ray Conference (ICRC2023)
26 July - 3 August, 2023
Nagoya, Japan

*Speaker

PoS(ICRC2023)245

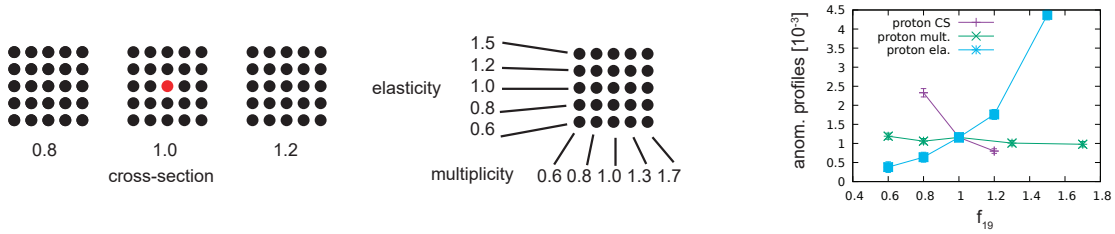

Figure 1: Left: In all the relevant plots, we use basic building blocks of 75 points to show the effects of the modifications. The red point shows where unmodified simulations are. Right: fraction of showers with anomalous longitudinal profiles for single-parameter modifications in CONEX.

1. Introduction

We investigate the effects of modified characteristics of hadronic interactions (MOCHI), namely the modification of three basic parameters – multiplicity, elasticity $\kappa_{\rm el} = E_{\rm leading}/E_{\rm tot}$ and cross-section – on the development of extensive air showers. These changes are implemented in CORSIKA 7.741 [1] using the CONEX option for the high-energy part of the showers, based on the work [2] with extensive modifications (we also use the original implementation in standalone Conex [3]). The modification of parameters is done without any reference to an underlying physical mechanism by changing the cross-section provided by an existing hadronic interaction model (Sibyll 2.3d [4] in our case) and resampling the secondary particles produced by the model to achieve the desired elasticity and multiplicity with the least possible change in other properties of the generated particles. The modifications for interactions of nuclei are implemented as modifications of the individual proton-air sub-interactions.

For each set of simulations, we select for each modified parameter a factor f_{19} and then for each interaction at an energy E above a threshold $E_{\rm thr}$, the parameter is modified by the factor

$$f(E, f_{19}) = 1 + (f_{19} - 1) \cdot \frac{\log_{10}(E/E_{\rm thr})}{\log_{10}(10\ {\rm EeV}/E_{\rm thr})} \qquad (1)$$

We consider 75 combinations of modifications: $f_{19}^{\sigma} \in (0.8, 1.0, 1.2)$ for cross-section, $f_{19}^{\rm el} \in (0.6, 0.8, 1.0, 1.2, 1.5)$ for elasticity and $f_{19}^{\rm mult} \in (0.6, 0.8, 1.0, 1.3, 1.7)$ for multiplicity. Thresholds are 10^{16} eV for cross-section, 10^{14} eV for elasticity and 10^{15} eV for multiplicity. (For further discussion, see [5]). For each combination, we simulate 1000 showers for the primary proton and 1000 showers for primary iron at a primary energy of $10^{18.7}$ eV and zenith angles $\theta \in (0, 25.7, 37.8, 48.7, 60)$ deg, totaling 750 thousand simulated showers. We call each set of 1000 simulations a "bin" for brevity, and we adopt a unified pattern for the visualization of the 75 modifications, see Fig. 1

2. Depth of maximum of energy deposit

While the extraction of the depth of the maximum of the energy deposit $X_{\rm max}$ from simulations is routine, care must be taken for the case of modified simulations for the following reasons:

1. The CONEX option in CORSIKA does not allow multiple observation levels. Thus, showers cannot be followed below the ground level of interest, which we set at 1400 meters a.s.l..

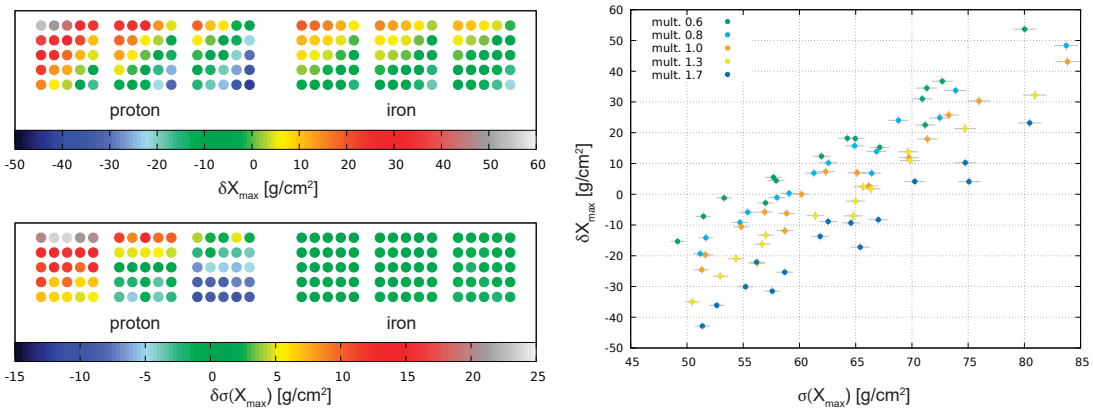

Figure 2: Left: changes in $X_{\max}$ and $\sigma(X_{\max})$ for different modifications, averaged over the three largest zenith angles. Right: correlation between $\sigma(X_{\max})$ and $X_{\max}$ is particularly strong for bins with the same change of multiplicity.

All simulated iron showers have a maximum above ground, but for proton showers, 10–40 % of showers for $\theta = 0°$ and up to 6 % of showers in each bin for $\theta = 25.7°$ have a maximum below ground (less than 1 % for unmodified showers). We use only the three largest zenith angles for $X_{\max}$ analysis. 2. Modified simulations can show a larger deviation from the typical shower profile, in particular when elasticity is increased. This leads to problematic results when fitting a Gaisser-Hillas function with constraints on its parameters X_0 and λ derived from unmodified simulations on the modified profiles. (Using an unconstrained Gaisser-Hillas is not helpful.) 3. A problem in the CORSIKA version used causes outlier points in the longitudinal profiles, which make it difficult to find the maximum by just searching for the highest point of the profile. For unmodified simulations, it affects a tiny fraction of showers; when elasticity and/or multiplicity is decreased, this becomes far more common, affecting more than 10 % of showers.

We algorithmically detected and removed showers affected by problems 2 and 3, but even when removing up to 18 % of showers in some bins, we still find large bin-to-bin fluctuations. The solution to both problems simultaneously is to calculate, for each shower, two values of $X_{\max}$ – one from a constrained Gaisser-Hillas fit within 100 g/cm^2 from the highest point and the other by finding the extreme of a parabola defined by three points around the highest point in the profile. A shower is rejected if these two maxima disagree by more than 20 g/cm^2; otherwise, the highest-point parabola $X_{\max}$ is taken, as this method has better stability with zenith angle. An exception is made for the small fraction of proton showers at 37.8 degrees with maxima underground, where the fitted value of $X_{\max}$ is taken instead. This method, while excluding less than 3.5 % of showers per bin, leads to consistent results.

For proton, the mean values of $X_{\max}$ (from the combined three largest zenith angles) and the standard deviation $\sigma(X_{\max})$ span a significant range of values (fig. 2), with some correlation. For a given multiplicity, the correlation is very high – changes in cross-section and elasticity only act along the line of the correlation. For iron, the effect on mean $X_{\max}$ is, on average, about 40 % of that for proton, but the effect on $\sigma(X_{\max})$ is much smaller, with $\sigma(X_{\max})$ for iron being always within 21–25 g/cm^2. The right panel of Fig. 2 also shows that while the statistical uncertainties

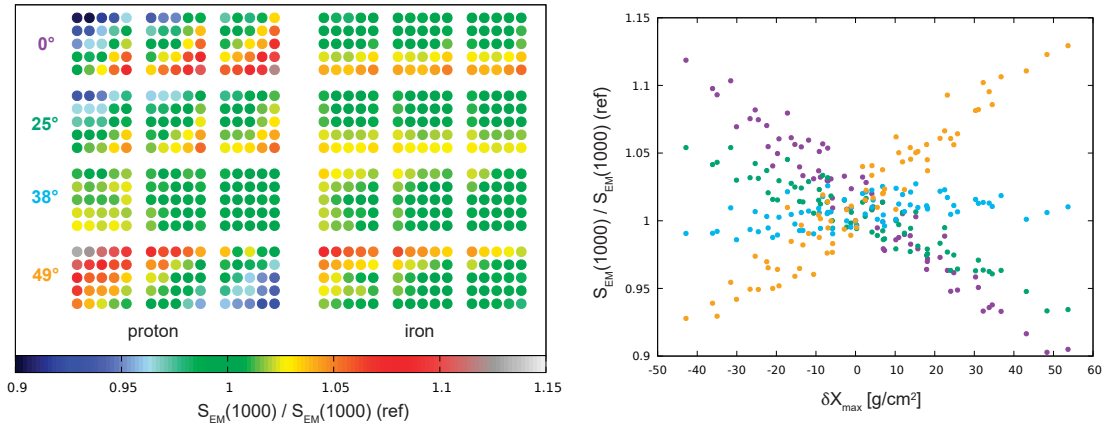

Figure 3: Left: relative change of EM signal at 1000 m for all relevant bins. Right: correlation with mean $X_{\max}$ shift for primary protons; different colors indicate different zenith angles, with colors indicated on the left panel; uncertainties in this and the following figures are omitted for clarity.

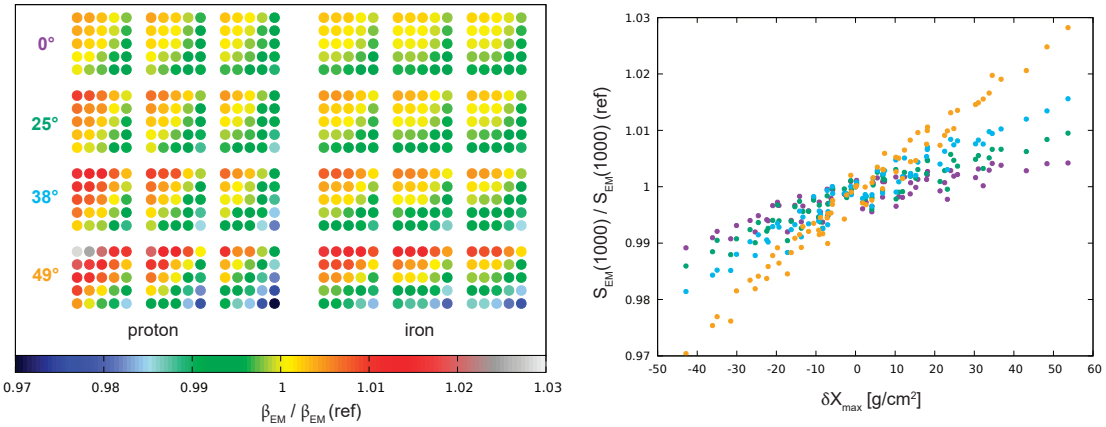

Figure 4: Left: relative change of the EM LDF slope β for all relevant bins. Right: correlation with mean $X_{\max}$ shift for primary protons; different colors indicate different zenith angles, with colors indicated on the left panel.

for mean $X_{\max}$ are negligible compared to the changes, for $\sigma(X_{\max})$, they are significant even with 3000 showers for each modification.

To study the effect of modified interactions on the profile shapes, we simulate additional showers in CONEX only with higher statistics – 2×10^5 showers per bin, but only for modifications of a single parameter, for proton primaries. We identify a shower as anomalous when the sum of absolute differences between the profile and a Gaisser-Hillas fit exceeds a threshold optimized on unmodified showers. This sum correlates well with the difference between the calculated χ^2 of this fit and of a fit using a sum of two Gaisser-Hillas functions, suggesting that most anomalous profiles have a significant distinct sub-shower. The fraction of anomalous showers depends strongly on cross-section but only weakly on multiplicity (fig. 1 right; elasticity to be added in the final version).

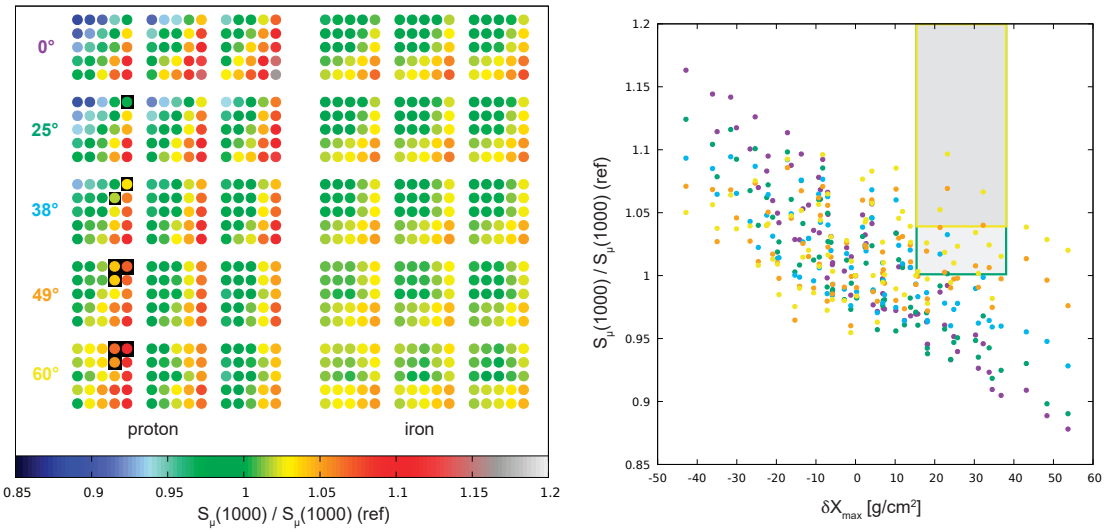

Figure 5: Left: relative change of muon signal at 1000 m for all relevant bins. Right: correlation with mean $X_{\max}$ shift for primary protons; different colors indicate different zenith angles, with colors indicated on the left panel; the shaded areas corresponds to the results of the Pierre Auger Observatory at $\theta = 55$ (yellow border) and $\theta = 28$ (green border)[10] and the modifications that fall within these areas for appropriate zenith angles are highlighted in the left panel.

3. Muon production depth

Unlike the longitudinal profiles of the electromagnetic component, the shape of the longitudinal profiles of the muon production depth (MPD) of muons that reach the ground is not universal [6]. The universality of the *total* MPD is distorted by the muon propagation and decay [7], meaning that the shape of the apparent MPD distribution, i.e., the one reconstructed from the muons reaching the detectors, shows a dependency on the zenith angle and adopted radial cut, being these effects less severe for the zenith angle region $\sim 60°$ [8]. For the reasons stated above, the fit of the maximum of the apparent MPD profile was performed with a universal shower profile (USP) fit [9], with all four parameters set free, since the USP fit is more stable than the one with a Gaisser-Hillas function. For the fitting procedure, we calculate the integral of the full distribution and make a set of fits ranging from an integral of around the first 5% up to 100% of the integral of the distribution. We then vary the fitting range around the maximum value of the profile and select the best fit according to its p-value. We reject all the cases where the MINUIT failed or the maximum fit value is below the ground. The results of the maximum of the MPD distribution $X^{\mu}_{\max}$ will be presented in the final version of these proceedings.

4. Ground observables

To suppress local fluctuations, for the EM component, we fit the energy density of EM particles as a function of radial distance (in the plane perpendicular to shower axis, between 300 and 1700 meters) with an NKG-like function $S_{\rm EM}(r) = N[(r/700)(1 + r/700)]^{-\beta_{\rm EM}}$ which describes the

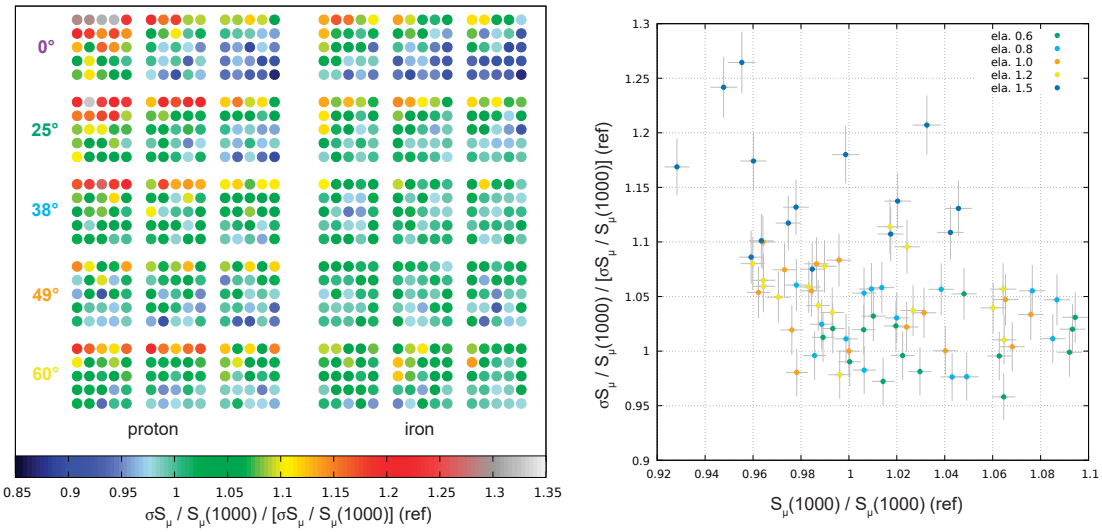

Figure 6: Left: relative change of relative fluctuations of muon signal at 1000 m for all relevant bins. Right: correlation with the relative change of in $S_\mu(1000)$ for primary protons for $\theta = 38$; different colors indicate different change of elasticity.

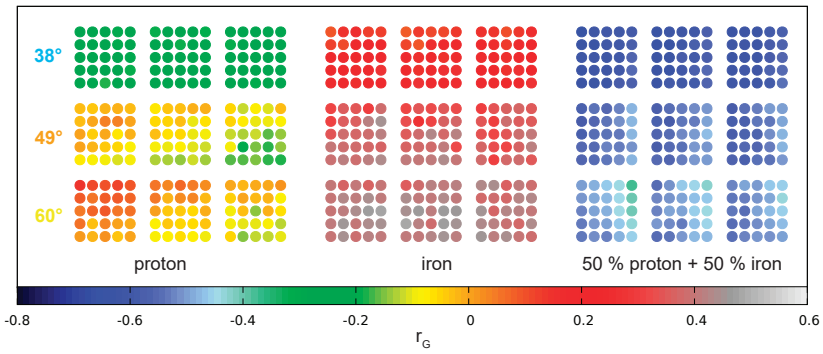

Figure 7: Ranking coefficient r_G for $S_\mu(1000)$–$X_{\max}$ correlation for proton, iron and mixed primary beams for the three zenith angles where full $X_{\max}$ coverage is available.

LDFs very well with just two parameters, except for $\theta = 60$ for which the EM component is small and we exclude it. We exclude only showers (no more than 5 per bin) where the fits are significantly worse. Figures 3 and 4 show the results for the ratios $S_{\mathrm{EM}}(1000)$ and β_{EM} to the respective values for unmodified simulations of same primary particle and θ, from which it is clear that the changes are dominated by the shifts in $X_{\max}$.

For the muon component, we have not found a two-parametric function that would properly describe the number density of muons for all bins and we thus fit $S_\mu(r) = N(r/320)^{-\alpha_\mu}(1 + r/320)]^{-\beta_\mu}$ with three parameters, which describes the LDFs well, but as α and β are degenerate, we use the ratio $S_\mu(500)/S_\mu(1500)$ to quantify the LDF slope instead. We find that the change of this slope is very tightly correlated with changes in $X_{\max}$ (with essentially the same slope for all values of θ except for 60 degrees). The change in $S_\mu(1000)$ is much less correlated with changes

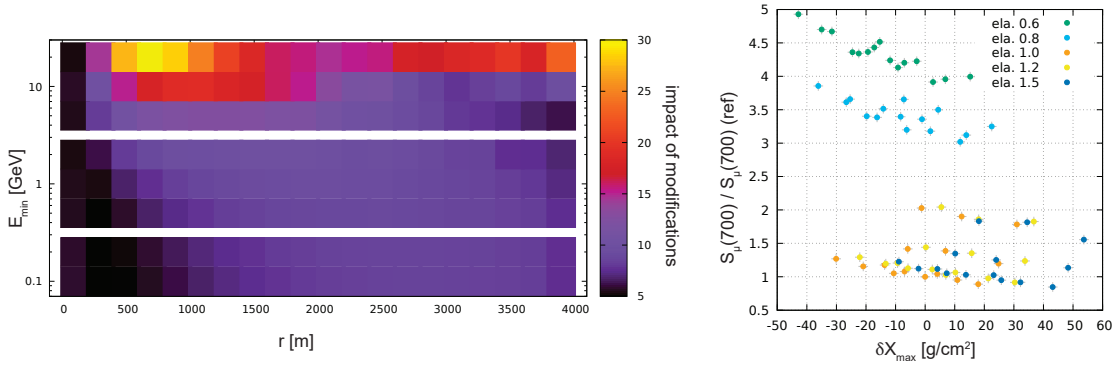

Figure 8: Left: impact of modifications on muon densities for different radial distance and $E_{\min}$. Right: S_μ–$X_{\max}$ plot for the most significant combination, colored by elasticity.

in $X_{\max}$, particularly for high θ, see fig. 5; in the right panel we also show what the Pierre Auger Observatory reports [10] as the most likely changes within systematic uncertainties. Two areas are shown - in bins centered at $\theta = 55$ (yellow border) and $\theta = 28$ (green border). We select our points at similar θ which lie within the respective boundaries and highlight them on the left panel. Note that with our modifications, it is easier to reproduce the Auger results at higher zenith angles.

The uncertainty in the relative fluctuations $\sigma S_\mu/S_\mu$ at 1000 meters at our statistics is high enough compared to their changes due to the modifications that this shows up as substantial noise in the left panel of fig. 6; the right panel illustrates these uncertainties and shows for a selected θ that the modifications allow relatively independent changes of $\sigma S_\mu/S_\mu$ and S_μ, with changes in the former being dominated by elasticity.

5. Combined observables

Having extracted well-defined values for $S_\mu(1000)$ and $X_{\max}$ for each shower (except for a small fraction that was excluded, see above), we use the Gideon-Hollister ranking coefficient r_G [11] to assess the correlation between the two variables. Fig. 7 shows that while modifications can make the correlation for pure proton approach that of pure iron, the large difference from values for highly mixed primary beam remains.

6. Sensitivity vs. muon energy and radius

Various scans can be performed to look for observables where the modifications have the largest effect. An example is shown in fig. 8 where we scan the muon signal (obtained as the average in a 200-meter thick annulus) as a function of radius and muon energy threshold. For each combination, we calculate the average over all modifications of the absolute difference of the muon density from the reference value divided by statistical uncertainty for 1000 showers. For the combination with the largest effect found ($r = 700$ m, $E_{\min} = 20$ GeV), we see on the right panel that particularly lowering the elasticity has indeed a huge effect for this observable. Measurements of high-energy muons could constrain the hadronic interactions of cosmic rays strongly.

Acknowledgements

This work is funded by the Czech Science Foundation GAČR 21-02226M.

References

[1] D. Heck, J. Knapp, J. N. Capdevielle, G. Schatz, and T. Thouw. CORSIKA: A Monte Carlo code to simulate extensive air showers. *FZKA-6019*, 1998.

[2] R. Ulrich, R. Engel, and M. Unger. Hadronic Multiparticle Production at Ultra-High Energies and Extensive Air Showers. *Phys. Rev. D*, 83:054026, 2011.

[3] T. Bergmann et al. One-dimensional Hybrid Approach to Extensive Air Shower Simulation. *Astropart. Phys.*, 26: 420–432, 2007.

[4] F. Riehn, R. Engel, A. Fedynitch, T. K. Gaisser, and T. Stanev. Hadronic interaction model Sibyll 2.3d and extensive air showers. *Phys. Rev. D*, 102(6):063002, 2020.

[5] J. Blazek, J. Vicha, J. Ebr, R. Ulrich, T. Pierog, and P. Travnicek. Modified Characteristics of Hadronic Interactions. *PoS*, ICRC2021:441, 2021.

[6] S. Andringa, L. Cazon, R. Conceicao, and M. Pimenta. The Muonic longitudinal shower profiles at production. *Astropart. Phys.*, 35:821–827, 2012.

[7] L. Cazon, R. Conceicao, M. Pimenta, and E. Santos. A model for the transport of muons in extensive air showers. *Astropart. Phys.*, 36:211–223, 2012.

[8] Lorenzo Cazon, R. A. Vazquez, and E. Zas. Depth development of extensive air showers from muon time distributions. *Astropart. Phys.*, 23:393–409, 2005.

[9] S. Andringa, R. Conceicao, and M. Pimenta. Mass composition and cross-section from the shape of cosmic ray shower longitudinal profiles. *Astropart. Phys.*, 34:360–367, 2011.

[10] J. Vicha for the Pierre Auger Collaboration. Adjustments to Model Predictions of Depth of Shower Maximum and Signals ... *PoS*, ICRC2021:310, 2021.

[11] R. A. Gideon and R. A. Hollister. A rank correlation coefficient resistant to outliers. *Journal of the American Statistical Association*, 82(398):656–666, 1987.